THE EFFECT OF WATER VAPOR ON COUNTERFLOW DIFFUSION FLAMES

by

Jaeil Suh and Arvind Atreya
Combustion and Heat Transfer Laboratory
Department of Mechanical Engineering and Applied Mechanics
The University of Michigan
Ann Arbor, MI 48109-2125

International Conference on Fire Research and Engineering, September 10-15, 1995. Orlando, FL. Proceedings. Sponsored by National Institute of Standards and Technology (NIST) and Society of Fire Protection Engineers (SFPE). D. Peter Lund and Elizabeth A. Angell, Editors. Society of Fire Protection Engineers, Boston, MA, 1995.

NOTE: **This paper is a contribution of the National Institute of Standards and Technology and is not subject to copyright.**

THE EFFECT OF WATER VAPOR ON COUNTERFLOW DIFFUSION FLAMES

JAEIL SUH AND ARVIND ATREYA

Combustion and Heat Transfer Laboratory
Department of Mechanical Engineering and Applied Mechanics
The University of Michigan, Ann Arbor, MI 48109-2125

Abstract

The chemical and physical effect of water vapor on the structure of counterflow diffusion flames is investigated both experimentally and theoretically. The experimental flame structure measurements consist of profiles of temperature, stable gases and hydrocarbons, soot and OH radical concentrations and spatially resolved radiative emission measurements. These experimental measurements are compared with numerical calculations with detailed C_2 chemistry. For these computations, experimentally measured temperature profiles were used instead of the energy equation to more accurately describe the flame radiative heat losses. The flame structure results show that as the water vapor concentration is increased, the OH radical concentration increases. This increases the flame temperature and the CO_2 production rate and decreases the CO production rate. However, after approximately 30% water vapor substitution, the chemical enhancement by water vapor is not observed and the flame temperature begins to decrease.

Introduction

Water has been, and is, the most important fire suppression agent. Currently, even though we have several other effective fire suppression agents, water is the most prevalent and the only agent for large fires because of its easy accessibility and non-toxicity. Water is supposed to behave as an inert in a fire, whereas, many chemical fire suppression agents are known to produce toxic compounds which restricts their usage. However, a lot of water is typically used to suppress a fire which causes severe water damage (sometime even more severe than the fire damage). To limit the water damage and to minimize the water usage, it is important to understand the mechanisms of fire suppression by water. Recently, there is considerable enthusiasm to use water mist as a substitute for halons and to reduce the water damage. This, however, requires the knowledge of adequate amount of water to efficiently suppress the fire. Thus, there is a need to quantify the effect of water on flames. Even though water has been used as a suppression agent for a long time, the exact mechanisms of fire suppression by water are not well understood.

Water is known to have two physical effects: (i) cooling of the burning solid by water evaporation and (ii) smothering caused by dilution of the oxidizer and/or the fuel by water vapor. These effects lead to fire suppression when water is applied to the fire. However, in addition to these effects, another effect of water which is not well known was observed and recently reported [1]. *This effect is the enhancement of chemical reactions inside the flames with water vapor.* Transient experimental results of reference [2] show an increase in the flame temperature, CO_2 production rate and O_2 depletion rate and a decrease in the CO and soot production rate with water substitution (fuel and oxidizer concentrations were held constant). These results are different from CO_2 substitution which reduced the flame temperatures and suppressed the fire. Thus, water substitution experiments suggest that the chemical reactions inside the flames are enhanced by water vapor.

In this paper, detailed structure of counterflow diffusion flames with water vapor is measured and calculated to investigate what occurs inside the flame and how the reactions are enhanced. The counter-

flow flame configuration was chosen because it represents the local behavior of large turbulent diffusion flames typical of fires. Measured temperature profiles were used for calculation to describe the flame radiation heat losses more accurately and the calculations were performed with the full C_2 mechanism.

Flame Temperature Measurements

For flame temperature measurement, the counterflow diffusion flame apparatus was used. Schematic of this apparatus is shown in Figure 1. The gap between the fuel side and the oxidizer side was 26mm and the radius of fuel and oxidizer exit was 38.1 mm and 63.5mm respectively. The flow rate of the fuel with diluent (nitrogen) through the fuel exit was 2 liter-per-minute, while that of the oxidizer with two different diluents (nitrogen and argon) was 8 liter-per-minute. The input concentration on the fuel side was 75% CH_4 and 25% N_2 and it was maintained constant for various water substitution to the oxidizer side flow. The input concentration on the oxidizer side was changed as water vapor was substituted, holding the molar concentration of O_2 constant at 20%. To maintain the same flow field and the same heat capacity of the oxidizer flow, a mixture of water vapor and argon was substituted for nitrogen. This maintained the same molar flow rate and roughly the same specific heat. Therefore the amount of oxygen which flowed into the flame was the same all the experiments (10, 20, 30 and 40% of water vapor substitutions). The flame temperature profile was measured with a coated S-type thermocouple (platinum and platinum with 10% rhodium). Silicone dioxide (SiO_2) coating was added and the measured temperature was corrected for radiation with simple calculation[3].

Computational Method

Numerical modeling of the chemical process is performed using *the Sandia Chemkin-based opposedflow diffusion flame code*[4]. The flame is modeled as a steady state opposed co-axial flow diffusion flame using the experimentally measured center line temperature profile. Pressure is assumed to be constant at 1 atm. The reaction mechanism for methane is C_2 -full mechanism which is consist of 177 chemical reactions with 32 species. More chemical reactions will be added later to account for chemical enhancement due to soot disappearance.

Governing Equations

Starting with the Navier-Stokes equations in cylindrical coordinates, stream function in the form $\Psi(x,r) \equiv r^2 U(x)$ is introduced[5]. For laminar stagnation point flow in cylindrical coordinates the mass

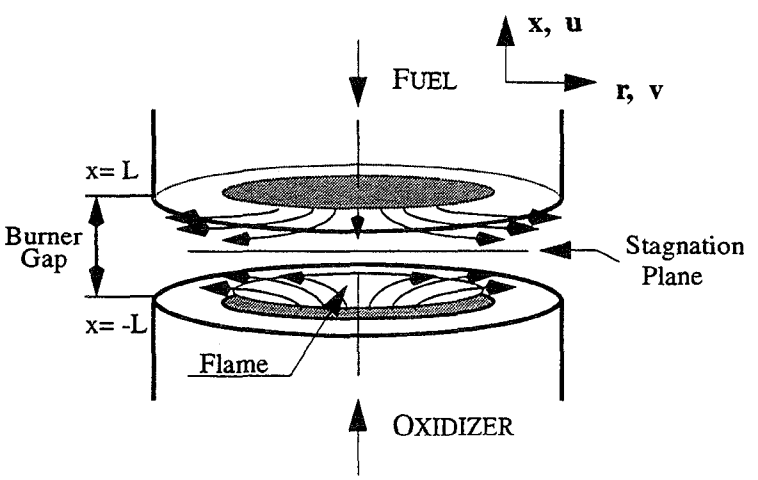

FIGURE 1. Schematic of the Counterflow Diffusion Flame Apparatus

conservation equation is expressed as follow.

$$\frac{\partial}{\partial x}(r\rho u) + \frac{\partial}{\partial r}(r\rho v) = 0 \tag{1}$$

Stream function, Ψ, satisfies this equation if it is defined as

$$\frac{\partial \Psi}{\partial r} = r\rho u = 2rU \tag{2}$$

$$\frac{\partial \Psi}{\partial x} = -r\rho v = r^2 \frac{dU}{dx} \tag{3}$$

from equations (2) and (3) it is clear that the axial velocity u depends only on x and the radial velocity v varies linearly in r.

$$u = \frac{2U}{\rho} \ (4), \quad v = -\frac{r}{\rho}\frac{dU}{dx} \ (5)$$

Assuming the temperature, T, and species mass fractions Y_k to be functions of x only and introducing these assumptions into the momentum equations without buoyancy, reduces the partial differential equations to third order ordinary differential equations, viz.

$$\frac{\partial P}{\partial x} = -4U\frac{d}{dx}\left(\frac{U}{\rho}\right) - 2\mu\frac{d}{dx}\left(\frac{1}{\rho}\frac{dU}{dx}\right) + \frac{4}{3}\frac{d}{dx}\left[2\mu\frac{d}{dx}\left(\frac{U}{\rho}\right) + v\frac{dU}{dx}\right] \tag{6}$$

$$\frac{1}{r}\frac{\partial P}{\partial r} = \frac{d}{dx}\left(\frac{2U}{\rho}\frac{dU}{dx}\right) - \frac{3}{\rho}\left(\frac{dU}{dx}\right)^2 - \frac{d}{dx}\left[\mu\frac{d}{dx}\left(\frac{1}{\rho}\frac{dU}{dx}\right)\right] \tag{7}$$

From the right hand side terms of equations (6) and (7), it is also clear that both $\frac{\partial P}{\partial x}$ and $\frac{1}{r}\left(\frac{\partial P}{\partial r}\right)$ are functions of x alone. Thus,

$$\frac{\partial}{\partial x}\left(\frac{1}{r}\frac{\partial P}{\partial r}\right) = \frac{1}{r}\frac{\partial}{\partial r}\left(\frac{\partial P}{\partial x}\right) = 0 \tag{8}$$

is derived and the only possibility which satisfy equation(8) is that $\left(\frac{\partial P}{\partial r}\right) = constant$. This is denoted by H, the radial pressure-gradient eigenvalue. Here, a new variable G is also introduced for convenience in equation(7).

$$G(x) = \frac{dU}{dx}$$

After substituting $G(x)$ into equation(7) and using k-species conservation equations and the energy equation, the boundary value problem that will be solved is summarized as:

$$\frac{dU}{dx} = G \tag{9}$$

$$\frac{d}{dx}\left[\mu\frac{d}{dx}\left(\frac{G}{\rho}\right)\right] - 2\frac{d}{dx}\left(\frac{UG}{\rho}\right) + \frac{3}{\rho}G^2 + H = 0 \tag{10}$$

$$2U\frac{dT}{dx} - \frac{1}{Cp}\frac{d}{dx}\left(\lambda\frac{dT}{dx}\right) + \frac{\rho}{Cp}\sum_{k=1}^{K} Y_k Cp_k V_k \frac{dT}{dx} + \frac{1}{Cp}\sum_{k=1}^{K} h_k \dot{w}_k = 0 \tag{11}$$

$$2U\frac{dY_k}{dx} + \frac{d}{dx}(\rho Y_k V_k) - W_k \dot{w}_k = 0 \ (k = 1 \ldots K) \tag{12}$$

The objective of the numerical method is find a solution for equations(9~12) with differential equation solver. In these equations k denotes k-th species, Cp is the constant pressure specific heat, h_k are species molar enthalpy, W_k are species molecular weights, Cp_k are constant pressure specific heat for each species and $\dot{w}_k$ are the chemical production rates. Transport properties, viscosity μ, thermal conductivity λ and species diffusion velocities V_k are also introduced.

Boundary Conditions

Boundary conditions for temperature, inlet velocity and the mixture compositions at the inlet of fuel and oxidizer (plug flow conditions) are specified as follows:

Fuel side: $x=L$

$$U_f = \frac{\rho_f \mu_f}{2} \quad , \quad G = 0 \quad , \quad T = T_f \quad , \quad Y_k = Y_{kf}$$

Oxidizer side: $x=-L$

$$U_o = \frac{\rho_o u_o}{2} \quad , \quad G = 0 \quad , \quad T = T_o \quad , \quad Y_k = Y_{ko}$$

Small symbol of f and o denote fuel and oxidizer. As stated earlier, for these calculations, measured temperature profiles were used instead of solving energy equation.

Results and Discussion

Measured temperature profiles for different water vapor substitutions are shown in Figure 2. The temperature profiles have the same shape except the peak temperature and the width. There is also a small shift in the location of the peak temperature for the 0% water case. We believe that the main reasons of this small shift is measurement error and/or change in properties (thermal and transport) of the oxidizer side of the flow with water vapor. Interestingly, the maximum temperatures of the flame are increased with the increase of water vapor substitution (1914K for 0% to 1960K for 40% water vapor) and the width of temperature profile is also increased. This means that water vapor which is added to the flame has other than a physical suppression effect. Figure 3 shows velocity profiles with different water vapor substitutions. All velocity profiles have nearly the same shape and the same stagnation plane location (8.3mm from the fuel exit), because inerts are substituted with water vapor on the same molar and heat capacity basis. Only in the highest temperature zones, the velocity profiles are different because of different heat release rates and transport characteristics of the mixture. Figures 4 and 5 show the concentration profiles for major stable species with 0% and 30% water vapor substitutions. They are all identical except water concentration because of water vapor substitutions. Figures 6 and 7 explains the effect of water vapor to the reaction of CO and CO_2. The concentration of CO_2 is gradually increased with increase of water vapor additions while the concentration of CO is decreased. The main reaction for CO_2 production with CO is as follows:

$$CO + OH = CO_2$$

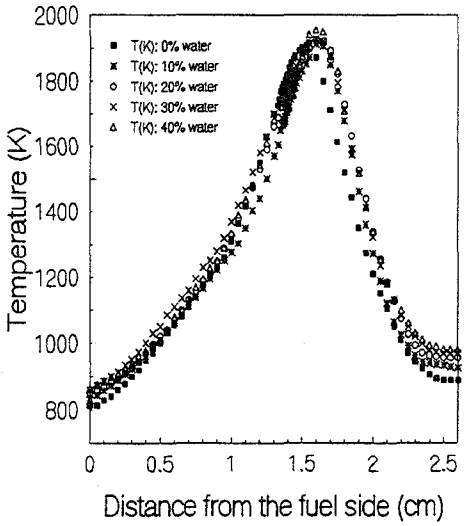

FIGURE 2. Measured Flame Temperature Profile

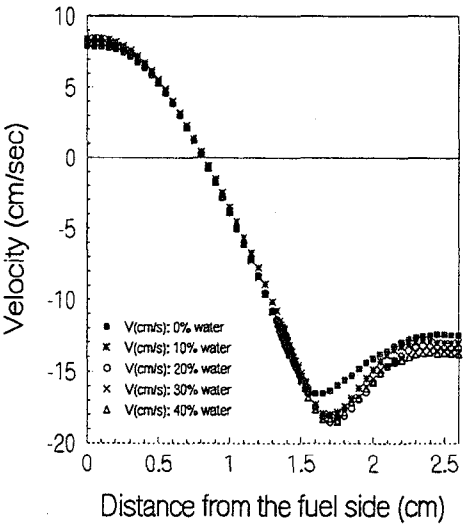

FIGURE 3. Calculated Velocity Profile

Therefore, the increase of CO_2 with decrease of CO means the active OH radical from water vapor which is produced in the high temperature flame zone enhances the reaction of CO to CO_2. Figure 8 shows the differences in the OH radical concentrations with and without water vapor addition. From Figure 8, it is clear that the presence of water vapor in the flame increases the OH concentration. There is, however, a limit to this OH concentration increase with increase in water vapor addition. Figure 9 shows the concentration of OH radical for various concentrations of water vapor. An increase in the amount of water vapor from 10% to 30%, OH radical concentration increases, but for the 40% water vapor addition case the concentration of OH radical stays almost as same as that of the 30% case. This result indicates that up to a certain amount of water addition (in this case it is between 30% and 40% of water vapor addition) the active OH radical concentration in the flame keeps increasing, but after this amount, increasing the water vapor concentration does not affect the OH radical concentration (we suspect that this will change if the O_2% is increased or the flame temperature is increased). This is the turning point of the chemical enhancement of water vapor to physical suppression effect on the flame. Another evidence of the turning point of the chemical effect is shown in Figure 10. Figure 10 shows the concentration of CH_3 radical with different water vapor concentrations. CH_3 is mainly produced by the following reaction, i.e. the first methane oxidation reaction.

$$CH_4 + H = CH_3 + H_2$$

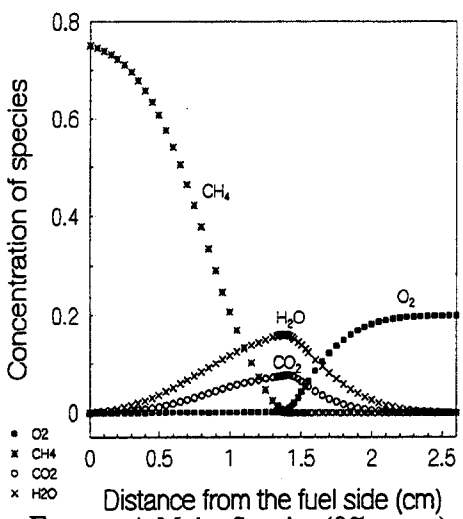

FIGURE 4. Major Species (0% water)

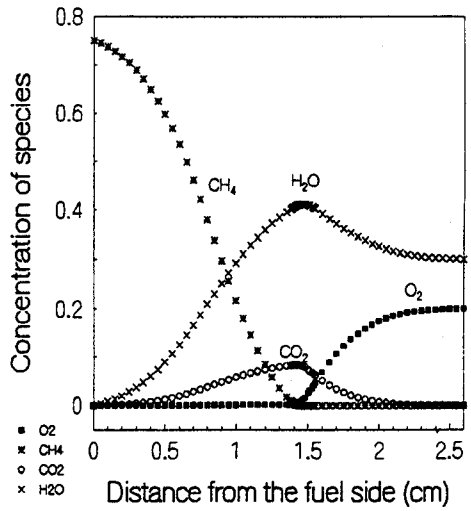

FIGURE 5. Major Species (30% water)

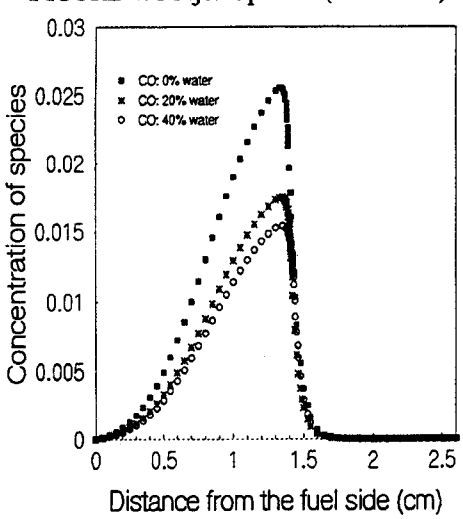

FIGURE 6. CO Concentration

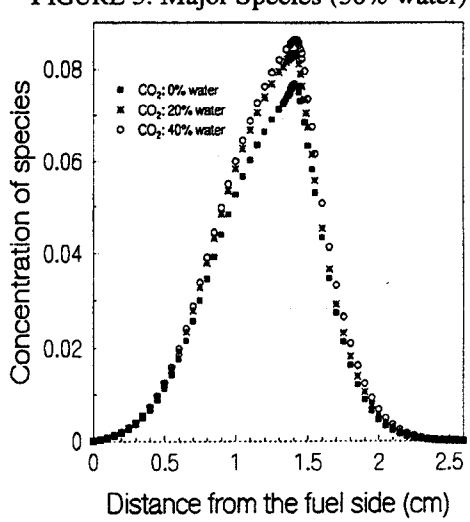

FIGURE 7. CO_2 Concentration

In the normal flame, 60% of H atoms react with CH_4 according to the above reaction[6]. Therefore an increase in the production of H atoms by water vapor addition increases the production of CH_3 and this indicates a more active flame. Figure 10 also shows that as the concentration profile of CH_3 is increased, its width increases with increase of water vapor substitution from 10% to 30%. However, for the 40% water vapor concentration case, the width of the CH3 decreases to a value between the 20% and 30% water concentration cases.

Conclusions

Computations of flame structure when water vapor is added to the counterflow diffusion flame using experimentally measured temperature profiles are performed for 5 different water vapor concentration cases. Maximum temperature and CO_2 production increased with an increase of water vapor concentration while CO concentration decreased. The concentration of OH radical increases with water vapor addition. This increase in the OH radical concentration explains CO_2 concentration increase and the maximum flame temperature increase. The turning point of the chemical effect to the physical effect of water vapor on the flame is found between 30% and 40% water vapor addition for this O_2% case. The concentration profiles of OH and CH_3 for various water vapor concentrations further substantiate the existence of this turning point where the effect of water on the flame changes from dominant chemical to dominant physical.

References

[1] Muller-Dethlefs, K., Schlader, A.F., *Combustion and Flame*, Vol. 27, pp.2050-215, 1976.

[2] Crompton, T., *Master thesis at University of Michigan*, 1995.

[3] Lee, K.C., "An Experimental Study on Soot Formation and Oxidation in Axisymmetric Counterflow Diffusion Flame," *Ph.D thesis at Michigan State University*, pp. 91-98, 1991.

[4] Kee, R.J., Miller, J. A., "A Structured Approach to the Computational Modeling of Chemical Kinetics and Molecular Transport in Flowing Systems," *Sandia National Laboratories Report*, SAND86-8841, 1992.

[5] Kee, R.J. Dixon-Lewis, G. et al., *Twenty Second Symposium (International) on Combustion*, pp. 1479-1494, The Combustion Institute, Pittsburgh, 1988.

[6] Westbrook, C.K., *Combustion Science and Technology*, Vol.34, pp. 201-225, 1983.

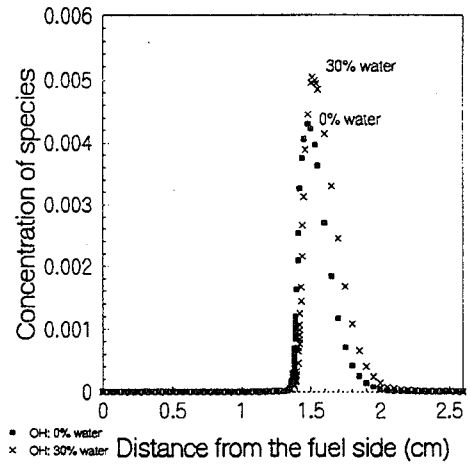

FIGURE 8. OH Concentration with & without water

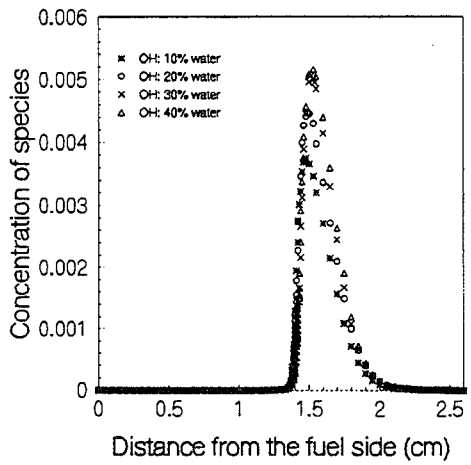

FIGURE 9. OH Concentration

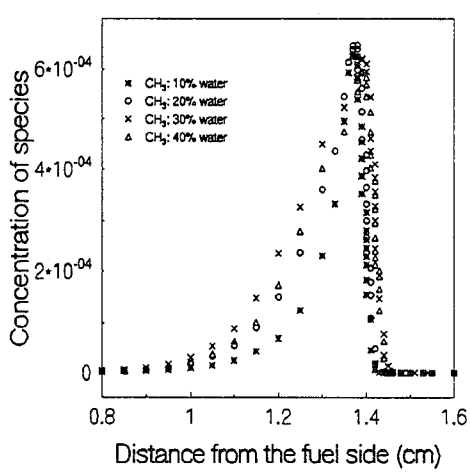

FIGURE 10. CH_3 Concentration